

## Local order in a supercooled colloidal fluid observed by confocal microscopy

This article has been downloaded from IOPscience. Please scroll down to see the full text article.

2003 J. Phys.: Condens. Matter 15 S375

(<http://iopscience.iop.org/0953-8984/15/1/351>)

View [the table of contents for this issue](#), or go to the [journal homepage](#) for more

### Download details:

IP Address: 171.66.16.119

The article was downloaded on 19/05/2010 at 06:25

Please note that [terms and conditions apply](#).

# Local order in a supercooled colloidal fluid observed by confocal microscopy

U Gasser<sup>1,3</sup>, Andrew Schofield<sup>2</sup> and D A Weitz<sup>1</sup>

<sup>1</sup> Department of Physics and Division of Engineering and Applied Sciences, Harvard University, Cambridge, MA 02138, USA

<sup>2</sup> Department of Physics and Astronomy, University of Edinburgh, Edinburgh EH9 3JZ, UK

E-mail: Urs.Gasser@uni-konstanz.de

Received 28 October 2002

Published 16 December 2002

Online at [stacks.iop.org/JPhysCM/15/S375](http://stacks.iop.org/JPhysCM/15/S375)

## Abstract

The local order in a supercooled monodisperse colloidal fluid is studied by direct imaging of the particles with a laser scanning confocal microscope. The local structure is analysed with a bond order parameter method, which allows one to discern simple structures that are relevant in this system. As expected for samples that crystallize eventually, a large fraction of the particles are found to sit in surroundings with dominant face-centred cubic or hexagonally close-packed character. Evidence for local structures that contain fragments of icosahedra is found, and, moreover, the icosahedral character increases with volume fraction  $\phi$ , which indicates that it might play an important role at volume fractions near the glass transition.

## 1. Introduction

The supercooling of liquids to temperatures well below their melting point is a well known and extensively studied subject. However, the microscopic processes that suppress the transition to the energetically more favourable crystalline phase are not well known. Often it is assumed that the predominant local structure in a supercooled liquid is of a non-crystallographic type, which cannot serve as a nucleation site for the crystalline phase and therefore makes it possible to reach a metastable region below the melting point. Frank [1] showed that the energy of an icosahedral (ico) cluster of 13 Lennard-Jones atoms is 8% lower than that of crystallographic clusters with 13 atoms (e.g. clusters with face-centred cubic (fcc) or hexagonally close-packed (hcp) arrangement of the 12 ligands). This gave rise to speculations that the predominant local order in supercooled liquids and glasses should be of the ico type, and that the supercooling of liquids would not be possible without this kind of non-crystallographic order.

The number of experimental results concerning the microscopic structure of supercooled liquids and glasses is still limited, because experiments providing information that goes beyond

<sup>3</sup> Present address: Fakultät für Physik, Universität Konstanz, D-78457 Konstanz, Germany.

averaged properties such as the pair distribution function  $g(r)$  are difficult with atomic or molecular systems. Therefore, most efforts to understand the question of the predominant local order in disordered materials have relied on computer simulations. Steinhardt, Nelson, and Ronchetti performed computer simulations of 864 Lennard-Jones atoms with periodic boundary conditions and reached the conclusion that the order is predominantly ico in the supercooled state [2, 3]. They observed that a state without translational symmetry but with extended orientational order begins to develop at a temperature 10% below the melting point. Furthermore, they speculated about frustration effects of the ico orientational order that might prevent the formation of a state with long-range ico order near the glass transition. For their analysis they developed local bond order parameter techniques that allow one to perform a kind of ‘spectroscopy’ of local structures. Sachdev and Nelson [4] developed a statistical mechanics theory for ico order in dense fluids, and they concluded that ico order should dominate in supercooled fluids. On the other hand, La Violette *et al* [5] found from computer simulations of the  $hx$ -model that icosahedra are scarce in the fluid. Moreover, according to their results, ico clusters have the highest energy among the clusters containing 13 atoms when they are embedded in the fluid. They used angle histograms of the triangles that are formed by neighbouring particles to analyse the local order. Finney and Wallace [6] analysed the local order in random packings of soft spheres with a Morse or Lennard-Jones potential by characterizing the interstices between the particles. For sufficiently soft potentials they found that only tetrahedral and octahedral interstices occur. From the arrangement of the interstices they concluded that the number of icosahedra is negligible.

## 2. Experimental details

The computer simulations mentioned above give some insight into local ordering that is very hard to observe experimentally in atomic or molecular systems, because the structures that are involved are very small and the timescales for the structural relaxations in liquids are very short. However, these difficulties can be avoided by using colloidal suspensions, which show a phase behaviour that is analogous to that of atomic materials.

In our experiments we used laser scanning confocal microscopy to study the local properties of supercooled fluids and crystals in a suspension of colloidal particles. Since the particles were large enough to be observed directly, it was possible to determine and track the position of each ‘atom’ for long times. The typical time for structural changes was quite long; the diffusion time  $\tau_s = a^2/D_s \sim 30$  s for our particles in a concentrated sample, where  $a = 1.21 \mu\text{m}$  is the radius of the particles. The time resolution of the experiment was always in the range between 30 and 45 s, and consequently the dynamics could be followed in detail. We used colloidal polymethylmethacrylate (PMMA) particles with a polydispersity <5% that were sterically stabilized with poly-12-hydroxystearic acid polymer grafted on their surfaces [7, 8] and that were fluorescently labelled with rhodamine in order to make them visible to fluorescence microscopy. The solvent was a mixture of decahydronaphthalene and cyclo-heptyl-bromide that matched the density and the index of refraction of the particles.

The poly-12-hydroxystearic acid polymer on the surface of the beads causes a strong repulsion when two particles get so close that their polymer layers begin to overlap, and since the electric charge of the particles is very small, the interaction is close to that of hard spheres. The samples used in this study had volume fractions between  $\phi = 0.42$  and  $\phi = 0.57$ . By comparison of the eventual phase behaviour of all samples (including additional samples above the glass transition), the melting point was determined to be close to  $\phi = 0.46$ , and the freezing point was close to  $\phi = 0.42$ . Compared to the phase diagram of hard spheres [9], the freezing and melting volume fractions were shifted from  $\phi_f^{HS} = 0.494$  and  $\phi_m^{HS} = 0.545$  to lower values, as expected for particles with a small charge.

Typically, the samples had a volume of  $\sim 30 \mu\text{l}$ , but only a  $50 \mu\text{m} \times 55 \mu\text{m} \times 20 \mu\text{m}$  volume was observed with a  $100\times$  objective with high numerical aperture by taking stacks of about 100 images. The distance between the images was  $0.2 \mu\text{m}$  in the vertical direction, and it took  $\sim 12 \text{ s}$  to take one snapshot of the whole volume. After removing noise with a typical size of one pixel from the images, the positions of the particle centres were determined with image analysis software that combines the information of all images [10]. Usually, the time resolution was good enough to track all particles.

### 3. Data analysis

The local order of the particles was analysed with a bond order parameter method [2, 3, 11]. First, the nearest neighbours of each particle were determined by using the minimum of the pair distribution function  $g(r)$  between the first and the second maximum as a cut-off distance. Then, each bond<sup>4</sup> was associated with a set of numbers  $\{Y_{lm}(\hat{r})\}$  ( $l = 4, 6$ ), where the  $Y_{lm}$  are spherical harmonic functions and  $\hat{r}$  is the unit vector parallel to the bond. The local surrounding of particle  $i$  was then characterized with the local bond order parameters  $q_{lm}(i) = (1/N_i) \sum_{j=1}^{N_i} Y_{lm}(\hat{r}_{ij})$  ( $l = 4, 6$ ), where  $N_i$  is the number of nearest neighbours of particle  $i$ . It has been shown that these local bond order parameters provide sufficient information about the local structure to discriminate between simple lattices such as fcc, hcp, body-centred cubic (bcc), and simple cubic (sc) [3]. Since the numbers  $q_{lm}(i)$  depend on the coordinate system, it is often of advantage to use rotational invariants of the  $q_{lm}(i)$ . We used the second-order invariants

$$q_l(i) = \left[ \frac{4\pi}{2l+1} \sum_{m=-l}^l |q_{lm}(i)|^2 \right]^{\frac{1}{2}} \quad (1)$$

with  $l = 4$  and  $6$  as well as the third-order rotational invariant

$$w_l(i) = \sum_{\substack{m_1, m_2, m_3 \\ m_1+m_2+m_3=0}} \begin{pmatrix} l & l & l \\ m_1 & m_2 & m_3 \end{pmatrix} q_{lm_1}(i) q_{lm_2}(i) q_{lm_3}(i), \quad (2)$$

with  $l = 6$ , which also contain enough information for a detailed analysis of the local structure [3, 11, 12]. Due to structural fluctuations, even in a purely crystalline phase there is a distribution of  $q_4$ ,  $q_6$ , and  $w_6$ . These distributions are characteristic for each structure, and they are used to quantify the particles that sit in a surrounding with the local structure considered.

### 4. Results and discussion

In an earlier study about the nucleation of colloidal crystals [12] we applied the local bond order parameter method that is described above and found that even the smallest crystal nuclei have strong fcc- and hcp-like character. However, the disorder is quite high, especially close to the solid–fluid surface, where neighbouring particles in the fluid phase lead to a fluid-like contribution in the histograms of the bond order parameters. Even during the early stage of nucleation no bcc-like order was found. These results were no surprise, since the equilibrium crystal phase for hard-sphere colloids is random hexagonal close packed (rhcp), which manifests itself as a mixture of fcc and hcp in the bond order parameter analysis.

Here, we concentrate on the particles in the fluid state and use again the rotationally invariant local bond order parameters  $q_4$ ,  $q_6$ , and  $w_6$  to characterize their local surroundings.

<sup>4</sup> In this context the word ‘bond’ does not denote a chemical bond but a direction or unit vector joining a particle with one of its nearest neighbours.

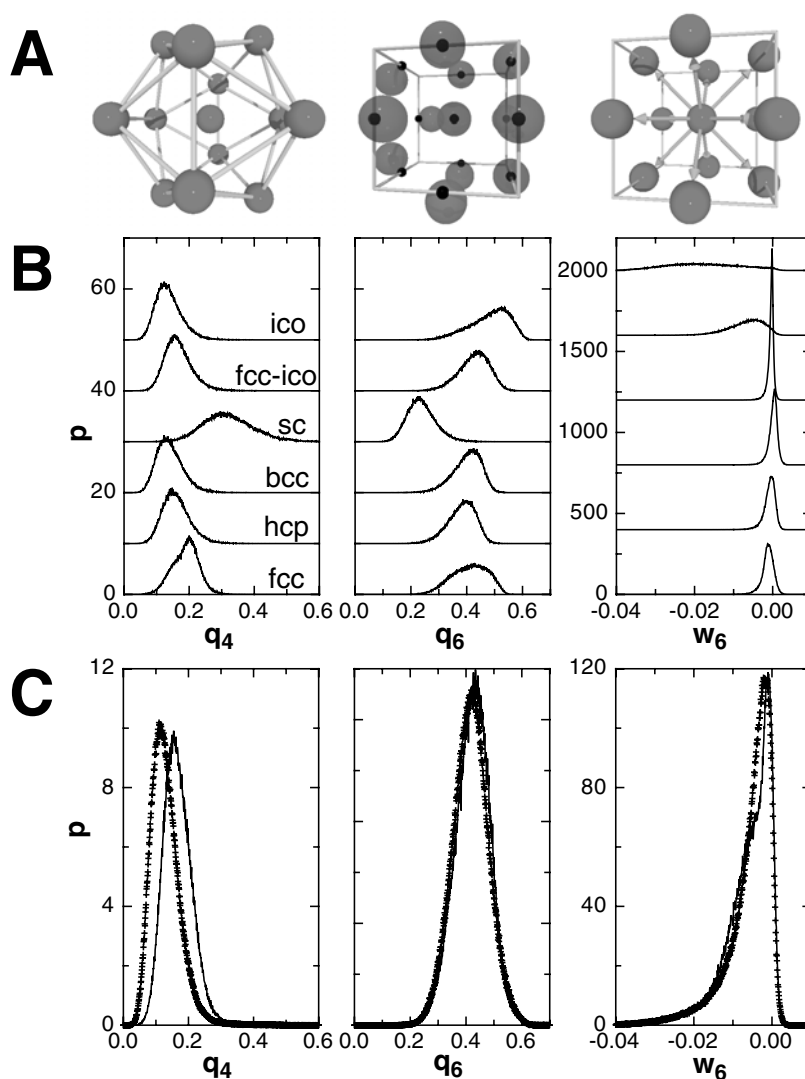


**Figure 1.** (A) ico, mixed fcc–ico, and fcc local structure (from left to right). The positions of the fcc–ico mixed local structure are represented by the large transparent spheres, while the smaller black spheres show the fcc positions for comparison. (B) Histograms of the local bond order parameters  $q_4$ ,  $q_6$ , and  $w_6$  are shown for (bottom to top) fcc, hcp, bcc, sc, mixed fcc–ico, and ico local order at  $\phi = 0.56$ . The histograms are offset by multiples of 10 ( $q_4$  and  $q_6$ ) and 400 ( $w_6$ ) for clarity. (C) Histograms of  $q_4$ ,  $q_6$ , and  $w_6$  obtained from the particles in the fluid state in a measurement at  $\phi = 0.56$  are shown by the symbols. The line shows a fit to the measurement with a linear combination of the bond order histograms from (B).

Again we look for particles with fcc-, hcp-, and bcc-like surroundings, but in addition we include sc, ico, and a combination of ico and fcc order in the analysis. As shown in figure 1(A), this combined local structure is a cluster with six particles on fcc and six particles on ico sites around a central particle. The histograms for the bond order parameters  $q_4$ ,  $q_6$ , and  $w_6$  for these structures are shown in figure 1(B); they were obtained from computer-generated particle coordinates for fcc, hcp, bcc, and sc lattices as well as from ico and mixed fcc–ico clusters at

the volume fraction of the sample considered ( $\phi = 0.56$ ). Random deviations were added to the ideal coordinates in such a way that the height and width of the nearest-neighbour peak of the measured pair distribution function  $g(r)$  was matched. From figures 1(B) and (C) it can be seen that fcc-, hcp-, and bcc-like surroundings have histograms that lie in essentially the same parameter ranges and have considerable overlap with the measured histogram, which is shown by the symbols in figure 1(C). The distributions of  $q_4$  and  $q_6$  for sc order, however, differ clearly from the measurement;  $q_4$  is too high and  $q_6$  is too low on average, and, therefore, sc local order can be excluded. The  $w_6$ -histograms for the ico and the mixed fcc–ico clusters are strikingly different from those of the other local structures. Therefore,  $w_6$  facilitates the detection of structures with ico character. Also, a comparison of the ico  $w_6$ -histogram with the measurement shows that no large number of well defined icosahedra can be expected, since the maximum of the ico  $w_6$ -histogram occurs at too low a value; this was found to be the case over the whole  $\phi$ -range that was examined in this study. The consideration of a mixed fcc–ico structure is motivated by the intermediate  $w_6$ -values that characterize such a combination of ico and close-packed order. Among the structures considered, only the  $w_6$ -histogram of the fcc–ico local order can account for the measurement in the range  $-0.025 < w_6 < -0.005$ .

The solid line in figure 1(C) shows a simultaneous fit with all three bond order parameters to the measurement with the linear combination  $\sum_i c_i h_i$  of the histograms in figure 1(B). Here,  $i$  stands for fcc, hcp, bcc, sc, fcc–ico, or ico,  $c_i$  is the contribution of the local order  $i$ , and  $h_i$  represents the  $q_4$ -,  $q_6$ -, and  $w_6$ -histogram of structure  $i$ . As expected, a considerable fraction of the measured histograms can be accounted for by the fcc and hcp histograms ( $c_{fcc} = 0.16 \pm 0.04$ ,  $c_{hcp} = 0.13 \pm 0.04$ ). Significant fcc and hcp contributions are not surprising, since, according to our earlier results [12], a large number of subcritical crystal nuclei with dominant fcc and hcp character formed in this measurement and because the sample crystallized eventually. The contributions from sc and bcc local order turn out to be negligible ( $c_{sc} = 0.000 \pm 0.001$ ,  $c_{bcc} = 0.000 \pm 0.001$ ). The  $w_6$ -histogram for bcc has its maximum at too high a value compared to the measurement. As expected, the fit also shows a large contribution from the mixed fcc–ico local order ( $c_{fcc-ico} = 0.64 \pm 0.02$ ). Also,  $c_{ico} = 0.08 \pm 0.03$ , since only ico local order can account for the  $w_6$ -tail at the lowest values ( $w_6 < -0.025$ ). However, overall the fit is not satisfactory, since a considerable fraction of the measured  $q_4$ -histogram at  $q_4 < 0.1$  is not accounted for. This shortcoming of the fit might be linked to the fact that only structures with the coordination number 12 contribute to the fit, while some particles in the measurement have less (15%) or more (19%) than 12 nearest neighbours.

Well defined icosahedra can be found by looking for particles with  $w_6 < -0.022$ . The cut-off value for the selection is somewhat arbitrary, since no sharp boundary between ico and other local structures exists. The numbers of particles that are found by this procedure to sit at the centre of an icosahedron is shown in figure 2. Their number is about a factor two to three lower than the bond order parameter fits suggest. The local volume fraction at the centre positions of the icosahedra was determined with the Voronoi construction and was found to be roughly 10% above the average  $\phi$ . Also, the icosahedra have the tendency to form small clusters or chains. The height of the first maximum of the pair distribution function  $g_{ico}(r)$  calculated with the centres of the icosahedra is larger than the first maximum of  $g(r)$  calculated with all particles: for the icosahedra the first maximum is in the range between 10 and 20, while the first maximum of  $g(r)$  grows from 3.67 ( $\phi = 0.43$ ) to 5.32 ( $\phi = 0.56$ ).

Although the number of particles with a well defined ico arrangement of their neighbours is relatively small, our bond order parameter analysis suggests that fragments of icosahedra are abundant; typically >50% of all particles in the fluid have bond order parameters that indicate a surrounding that is close to a fragment or a whole icosahedron. Therefore, fragments of

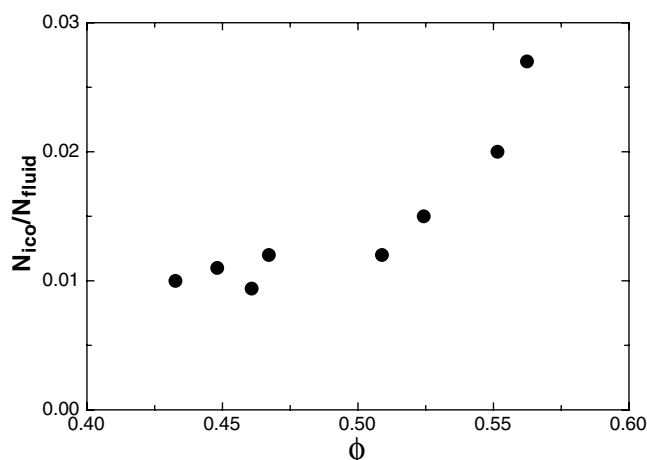


**Figure 2.** The fraction of particles in the fluid that was found to be icosahedrally coordinated in measurements at different volume fractions  $\phi$ . The icosahedra were identified by looking for particles with  $w_6 < -0.022$ .

icosahedra or distorted icosahedra might be important for a detailed description of the structure of the fluid. Moreover, the ico character of the local order increases with  $\phi$ ; this suggests that it might play an important role for  $\phi$  near the glass transition, as was suggested in [3]. Also, the tendency of the icosahedra to form clusters indicates that larger clusters with non-crystallographic symmetries might be present at volume fractions close to the glass transition. However, these clusters are probably not as large and well defined as those that were proposed by Hoare [13, 14].

## References

- [1] Frank F C 1952 *Proc. R. Soc. A* **215** 43–6
- [2] Steinhardt P J, Nelson D R and Ronchetti M 1981 *Phys. Rev. Lett.* **47** 1297–300
- [3] Steinhardt P J, Nelson D R and Ronchetti M 1983 *Phys. Rev. B* **28** 784–805
- [4] Sachdev S and Nelson D R 1985 *Phys. Rev. B* **32** 1480–502
- [5] La Violette R A and Stump D M 1994 *Phys. Rev. B* **50** 5988–98
- [6] Finney J L and Wallace J 1981 *J. Non-Cryst. Solids* **43** 165–87
- [7] Antl L *et al* 1986 *Colloids Surf.* **17** 67
- [8] Phan S-E, Russel W B, Cheng Z, Zhu J, Chaikin P M, Dunsmuir J H and Ottewill R H 1996 *Phys. Rev. E* **54** 6633–45
- [9] Alder B J and Wainwright T E 1957 *J. Chem. Phys.* **27** 1209
- [10] Crocker J C and Grier D G 1996 *J. Colloid Interface Sci.* **179** 298
- [11] Rein ten Wolde R, Ruiz-Montero M J and Frenkel D 1996 *J. Chem. Phys.* **104** 9932
- [12] Gasser U, Weeks E R, Schofield A, Pusey P N and Weitz D A 2001 *Science* **292** 258–62
- [13] Hoare M 1976 *Ann. NY Acad. Sci.* **279** 186–207
- [14] Hoare M R 1978 *J. Non-Cryst. Solids* **31** 157–79